Journal of Thermal Analysis, Vol. 36 (1990) 1519-1543

SINGLE RUN HEAT CAPACITY MEASUREMENTS
II. Experiments at subambient temperature

*Y. Jin** and *B. Wunderlich*

DEPARTMENT OF CHEMISTRY, UNIVERSITY OF TENNESSEE, KNOXVILLE, TN 37996-1600 AND CHEMISTRY DIVISION, OAK RIDGE NATIONAL LABORATORY, OAK RIDGE, TN 37831-6197, USA

(Received March 3, 1990)

A prior study of single-run differential scanning calorimetry that leads directly to heat capacity results is extended to low temperatures (180 K). The instrument considered was the duPont dual sample differential scanning calorimeter with auto sampler and liquid nitrogen cooling accessary-II. The major error is caused by the low temperature isotherm. After optimizing all parameters, heat capacities of selenium, aluminum, quartz, polystyrene, sodium chloride were measured between 180 to 370 K. The root mean square error of all measurements on comparison with well established adiabatic calorimetry is ± 2.9%.

In the previous paper [1] a study of single-run heat capacity measurements from 348 to 549 K was presented. These measurements were based on a prior mathematical model that showed feasibility of the approach [2]. The equipment used for the study was the duPont dual sample differential scanning calorimeter. We found at that time that the major errors were caused by environmental fluctuations. All other errors analyzed seem to permit an accuracy of ±0.3%.The overall root mean square error of all reported measurements, when compared to established adiabatic calorimetry was ±0.8%.

In this second experimental paper new results for the low temperature range 180 K to 370 K are presented with a detailed error analysis. In addition, some general experiences on this instrumentation are discussed.

*On leave from the Dept. of Material Science, Fudan University, Shanghai, China.

John Wiley & Sons, Limited, Chichester
Akadémiai Kiadó, Budapest

Again, all measurements were made with the duPont 2100 Thermal Analyzer System with a 912 Dual Sample Differential Scanning Calorimetry (DSDSC) cell, governed by an Auto Sampler (AS) and the Liquid Nitrogen Cooling Accessory-II (LNCA-II). Unless stated specifically, the work followed closely the research outlined in the prior paper [1]. The following effects were studied: baseline noise at different temperatures, baseline repeatability, asymmetry of the calorimeters, temperature lag, effect of pan type, cell constant, effect at heating rate differences between sample and reference. After optimizing the instrument, heat capacity measurements of five well-known samples were carried out and compared with literature data (Se, Al, SiO_2, polystyrene and NaCl). No additional information needed to be generated for crosstalk, the effect of nitrogen gas flow, the effect of pan weight and pan position [1].

Experimental

Instrumentation

The commercial equipment listed in the Introduction was used for thermal analysis of all samples. The instrument was controlled by an IBM PS/2 Model 60 computer through the module interface supplied by the duPont Co.

Before measurements, the DSDSC was adjusted by hardware and software as suggested by the manufacturer. Since full use of mathematic data analysis was made by our own software [3], uncorrected data were also collected. The adjustment of the baseline drift and cell constant by instrument calibration is preliminary except for the two-point temperature calibration by instrument software.

Indium, water and acetone were used as temperature calibration standards (melting points = 429.8 K, 273.2 K and 177.9 K, respectively). Sapphire was used as heat capacity calibration standard. All samples were encapsulated in standard aluminum pans (nonhermetically crimped pans).

All mass determinations were carried out on a Cahn electrobalance with a sensitivity of 0.01 mg and an overall accuracy of better than ±0.1 %. No nitrogen gas was purged through the DSC cell during subambient experiment since it could be shown to significantly increase the baseline noise.

For temperature calibration, an indium, water, or acetone sample was measured at different heating rates (1, 5, 10, 20 and 40 deg/min). The data were collected with different sampling intervals according to the heating

rates (about 0.1 deg/point) and stored on hard disk for further analysis. For heat capacity measurements, an empty pan, a sapphire standard and the unknown sample were placed on the three measuring positions of the DSDSC. All aluminum pans masses were adjusted to within ± 0.1 mg of each other.

A typical DSC run was carried out as follows: 1. The liquid nitrogen cooling was begun until the DSC cell reached the desired initial temperature. 2. With continued liquid nitrogen feeding the data storage was turned on, and an isotherm collected for the length of time needed to have a stable baseline. 3. The liquid feeding was stopped and the linear programmed heating started. The heating was stopped when the DSDSC cell reached the desired final temperature. 4. A final isotherm was collected. A typical example had an initial isothermal of 30 minutes at 173 K, was heated at 10 deg/min to 373 K, and then, a final isotherm was collected for 5 minutes at 373 K. The data were stored on the computer disk with sampling interval of 3.0 s/point or 0.5 K/point. The heat capacity calculations were done subsequently from the recorded amplitudes. The rate of feeding of the liquid nitrogen was controlled by the HEATER and RATE switches of the control head assembly of the LNCA-II. The greater the power of the heater, the greater is the cold nitrogen gas pressure and the faster can the device cool and the lower is the ultimate temperature. The amount of overlap in the activation of the analysis module heaters and the supply of coolant from the LNCA-II is set with the RATE dial (heater Bias Rate from 0 to 100 %). Low heater bias rates conserve liquid nitrogen, but allow less control of temperature, while high rates provide closer temperature control at the cost of increased use of liquid nitrogen. Obviously, when cooling down, fast cooling is more important (HEATER = 3 and RATE = 0%). When isothermal temperature control more important, the settings are changed to HEATER = 2 or 1, and RATE = 100%. In this case, the LNCA-II switches are adjusted manually. On automatic runs HEATER and RATE must be set at fixed positions. The compromise is HEATER = 2 and RATE = 50%.

Materials used

A sapphire disc and indium were supplied with the accessory kits of the DSC instruments. In addition, granular sapphire of about 1 mm diameter, traced to the original calorimetry was supplied by NIST, Gaithersburg, MD. Aluminum and selenium pellets of 99.999% purity were obtained from Aldrich Chem. Co., Milwaukee, WI. Sodium chloride of analytical reagent grade was acquired from Mallinckrodt Co., Paris, KY. A standard sample of polystyrene of MW = 100.000, $M_w/M_n < 1.06$ was bought from Polyscience,

Inc., Warrington, PA. The quartz used in this work was pure, supplied by the University glassblower in suitable shape.

Results and discussion

A. Adjustment of the instrument

1. Baseline slope

The LNCA-II permits a run to start from a temperature as low as 123 K. Figure 1 shows a typical result for a baseline scan at 123 K (no pans on any of the three positions). It is obvious that linear programmed heating can be controlled from 123 K, but there is an excessive baseline curvature (17 mW from 123 K to 373 K), and there is no steady state reached at the 123 K isotherm. The baseline curvature, could not be improved significantly by hardware adjustment of the baseline slope. Using the triple-cell approach there was still hope that internal calibration could eliminate the baseline

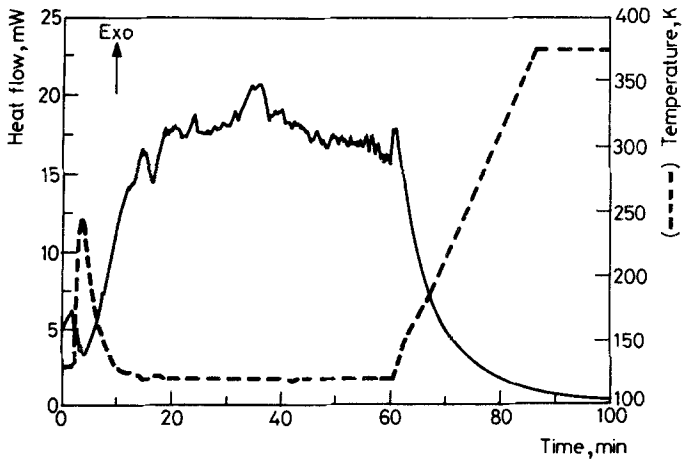

Fig. 1 A typical example for a baseline scan from 123 to 375 K at 10 K/min heating. Solid line: heat flow; dashed line: temperature

curvature between the two measuring cells. For any precise measurement, a reproducible isotherm is, however, necessary. Even after long times at 123 K the isothermal baseline would not settle to a steady state, but show short-time noise and long-time fluctuations as shown in Fig. 1. Extended efforts were made at optimizing all the parameters of the LNCA-II control, the

DSC heat proportional band, and the environment effect. Even measuring attempts on cooling instead of heating were tried, but none permitted to stabilize the baseline at 123 K.

After the poor isotherm performance at 123 K was accepted, an attempt was made to map the isotherms in steps up to the beginning of the prior studied high temperature range (323 K). Figure 2 shows 60 minute isotherms, interrupted by 10 deg/min cooling from 323 K to 123 K in steps of 50 K. One can see clearly that as the temperature decreases, the isothermal baseline becomes less stable and more noisy. The peak-to-peak baseline noise doubles approximately for every 50 K temperature decrease. (0.028 mW, 0.04 mW, 0.11 mW, 0.25 mW, and 0.55 mW at 323 K, 273 K, 223 K, 173 K and 123 K, respectively.) The stability seems sufficient down to about 173 K. Two attempts of measuring from 173 K are illustrated in Figs 3 and 4 for cells *A* and *B*, respectively. The DSC curves refer to two runs each on the same position of cell. One with an empty aluminum pan and the other a sapphire disc sealed in the same mass of aluminum pan. The isothermal baselines are sufficiently good, and matched between the empty and sapphire runs, both at 173 K, and at 373 K. Going stepwise to lower temperatures showed sufficient loss of repeatability of baseline that all further work is restricted to a starting temperature of 173 K, and since it takes at least 5 K to reach steady state on heating at 10 deg/min, heat capacities are reported starting from 180 K.

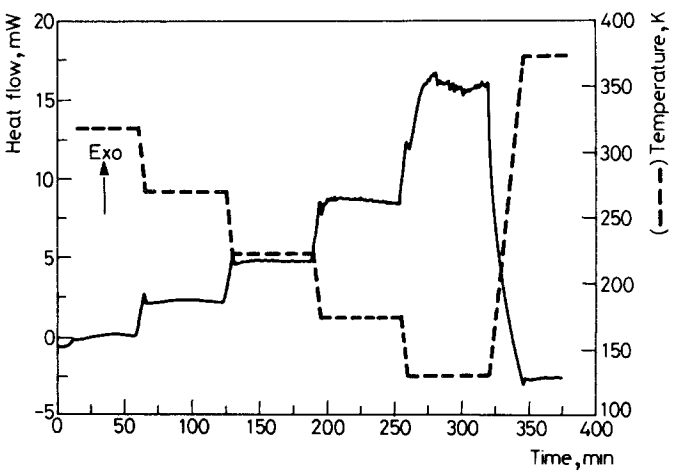

Fig. 2 DSC baseline performances at different temperatures with 60 min isotherms, interrupted by 10 K/min cooling from 323 to 123 K in steps of 50 K, and finally followed by 10 K/min heating from 123 to 323 K. Solid line: heat flow; dashed line: temperature

2. *Baseline repeatability*

The baseline repeatability was checked by placing three empty aluminum pans on the three positions of the DSDSC cell. The experiment was then run

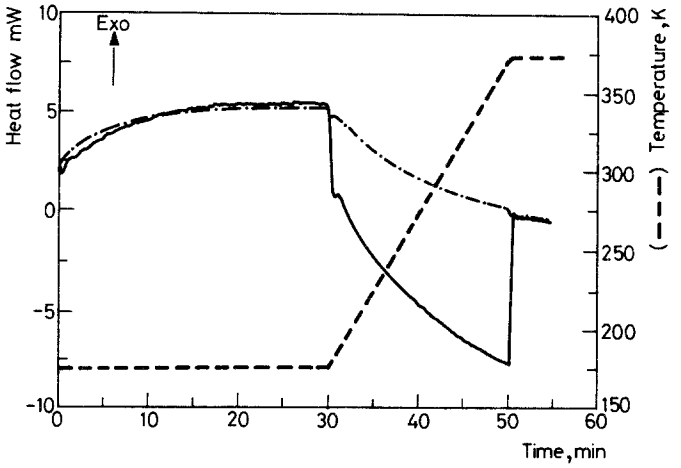

Fig. 3 A typical example in a time-based graph of heat capacity measurement on cell *A*. Solid line: sapphire in an aluminum pan; dash-dotted line: aluminum pan only; dashed line: temperature

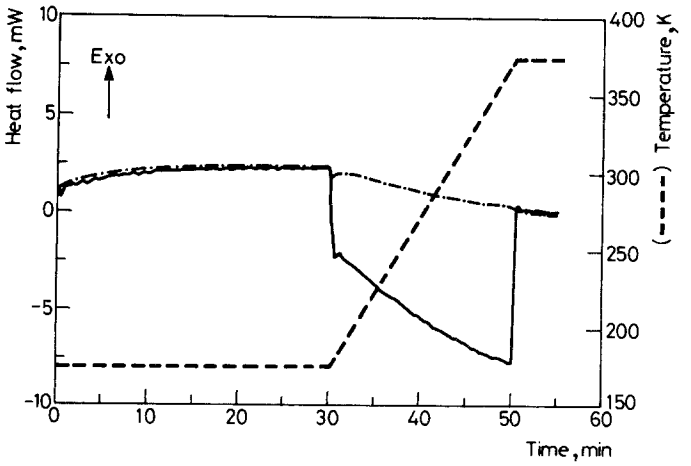

Fig. 4 Heat capacity measurement as in Fig. 3, but for cell *B*

as follows: start feeding liquid nitrogen and cooling to 173 K, record an initial isotherm of 30 minutes at 173 K; stop feeding liquid nitrogen and begin programmed heating at 10 deg/min to 373 K; then collect a final isotherm of 5 minutes at 373 K. This was followed by four repetitions of the initial run. The results are displayed in Figs 5 and 6 for cells *A* and *B*, respectively. The curves shifted with time, and the maximum fluctuations about the mean were ±0.6 mW for cell *A* and ±0. mW1 for cell *B*. For anyone set, the fluctuations could be reduced by matching the initial and final isotherms, i. e. the curves were off-set by a constant amount during the overall experiment, as can be seen from Figs 5 and 6. Correcting by matching the initial and final isotherms, the baseline repeatability was about ±0.1 mW for cell *A* and ±0.04 mW for cell *B*. If the amplitudes of an unknown sample were 10 mW, the baseline error could thus be reduced to about 0.4 to 1.0 %.

3. Single-run C_p measurement

Unlike C_p measurements at high temperature which were shown in the previous paper [1], we could not adjust the initial and final isotherm to the same horizontal level for DSDSC at low temperature. Obviously, without any calibration or without matching curves between empty and sample mass, it is not possible to get correct data from single-run C_p measurement because of the excessive baseline curvature of the empty pan and sample runs (Figs 3 and 4). The asymmetry of the cells *A* and *B* and its dependence on the cell constants and baseline curvatures, will be discussed below. At that point information is given on how to improve measurements by using curve matching between empty and sample runs, as well as asymmetry corrections of the C_p calibration constant. Finally, even further improvements are considered involving corrections for temperature lag and heating rate differences between sample and reference.

4. Symmetry of cells A and B

4.1 Baseline

Figures 5 and 6 show the different curvature on linear programmed heating as well as different initial and final isotherm levels for the identical empty pans on cells *A* and B, respectively. That means there is strong asymmetry between cells *A* and *B*. This asymmetry seems inherent in the present design and an effort should be made by the manufacturer to correct the problem. In the meantime, the best way to correct this asymmetry is to

match the isotherm of a calibration run of empty pans with the sample run (sample plus the same mass empty pan) at the initial and final temperatures (see Figs 3 and 4). The corrected amplitude of the sample run is obtained by subtracting the amplitude of the empty run from the sample run. This is a basic correction for the single-run C_p measurements. Other corrections need to be added for high precision measurement.

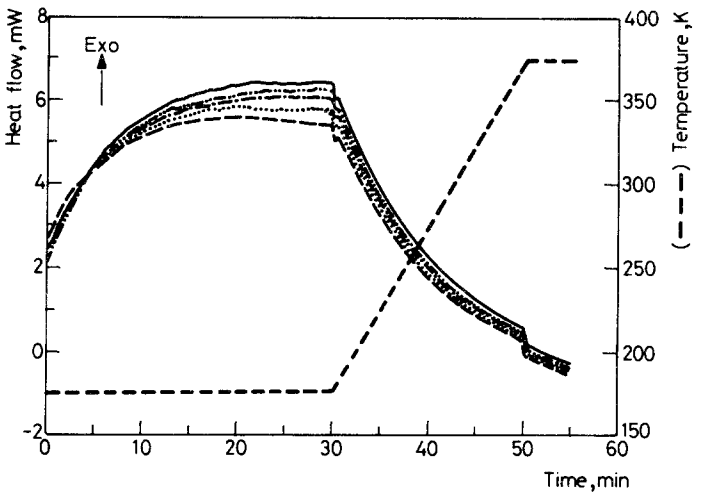

Fig. 5 Baseline repeatability of cell *A*. Short dash: temperature, others: heat flow of 5 successive runs

4.2 Cell constant

The cell constant is the calibration coefficient of the heat flow signal. Its value, normally close to 1.0 (dimensionless), should be determined for each particular DSC cell.

There are two ways to evaluate the cells constant. One is the ratio of the known to experimental heats of fusion by using a standard sample (e.g. indium ΔH_f = 28.42 J/g [4]):

$$\text{Cell constant} = \Delta H_{\text{standard}} / \Delta H_{\text{measured}} \quad (1)$$

The other is from the ratio of the known to the experimental heat capacity by using a standard sapphire sample:

$$\text{Cell constant} = C_{p\ \text{standard}} / C_{p\ \text{measured}} = C_{p\ \text{standard}} \times q \times \text{W}/(60 \times \text{A}) \quad (2)$$

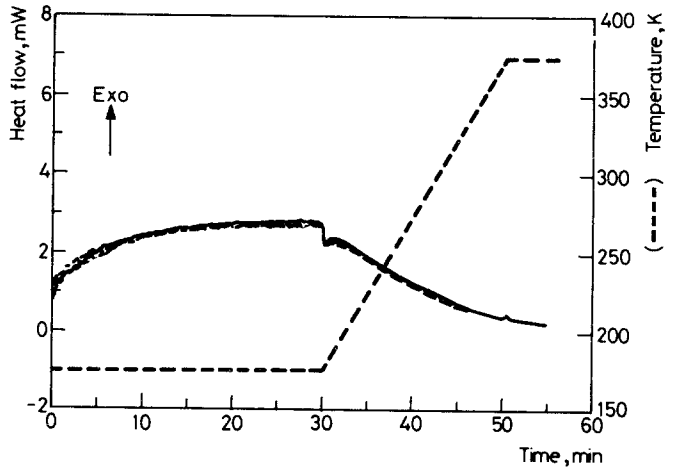

Fig. 6 Baseline repeatability of cell *B*, as in Fig. 5

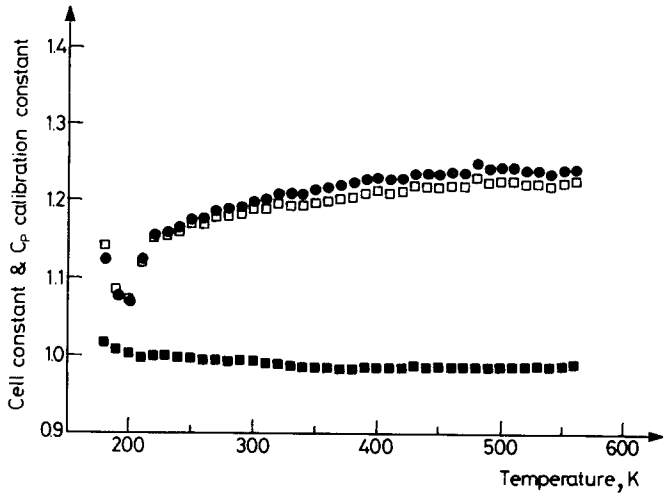

Fig. 7 Cell constants of cells *A* and *B* and calibration constant of heat capacity between cells *A* and *B*. open squares: cell constant of cell *A* (K_A); circles: cell constant of cell *B* (K_B); filled squares calibration constant of heat capacity (K_A/K_B)

In the second part of Eq. (2), q is the heating rate in deg/min, W is the sapphire sample mass in mg, the value of 60 is the conversion factor from

minutes to seconds, and A is the corrected heat flow amplitude in mW caused by the sample at the temperature of interest.

Equation (1) is used by duPont DSC as internal calibration and can give a calibration at only one temperature. For higher accuracy, Eq. (2) must be used. We developed the necessary software to get the cell constant for all temperatures from one sapphire standard sample run.

For calibration we used two standards with almost the same mass of aluminum pan, cover and sapphire disc (one as the standard, the other as the unknown samples). Figure 7 shows the cell constants K_A and K_B for cells A and B, as well as the heat capacity calibration constant between cell A and B as a function of temperature ($K = K_A/K_B$). One can see that K_A and K_B are changing with temperature, especially at low temperature, and also that there is a 2-3% difference between K_A and K_B which is caused by the asymmetry of the DSDSC cell. The asymmetry and the calibration constant were almost constant with temperature as shown in Fig. 7, and also with time and environmental changes. This means even if the cell constant changes (occasionally as much as by 10%) the C_p calibration constant is still constant within about ± 1.5%. In this fact lies the advantage of the dual sample DSC cell for heat capacity measurement. Figure 8 shows a plot of the calibration constants repeated 15 times within a time period of 2 months. Again the low

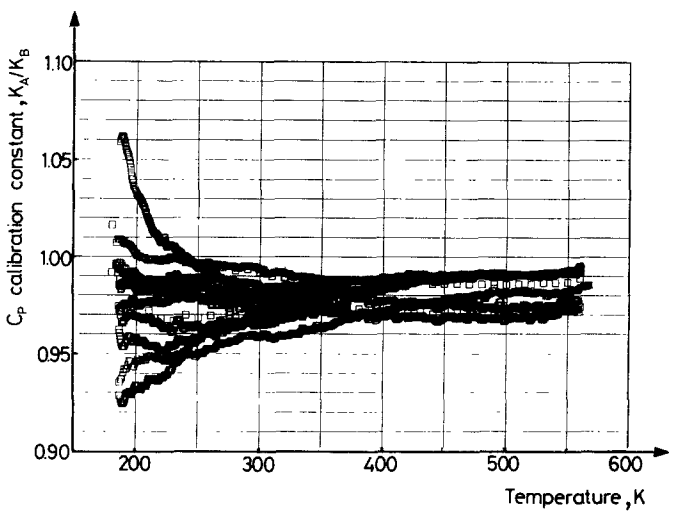

Fig. 8 Calibration constants of heat capacity repeated 15 times within a time period of 2 months. Average and RMS: 0.9780±0.0144

temperature repeatability is less than the high temperature repeatability. The average and RMS of the calibration constant was 0.9795 ±0.0160 for the low temperature range (180-373 K), and 0.9780 ±0.0144 overall (180-567 K).

5. Temperature lag corrections

For the heat capacity at low temperature, two additional temperature calibration standards, water and acetone, were used. All standards show similar melting point dependencies on the heating rate. We also compared the performance of the hermetically sealed pan to the non-hermetically sealed pan. It seems that the hermetically sealed pan causes a larger temperature lag than the non-hermetically crimped pan. Figure 9 shows the

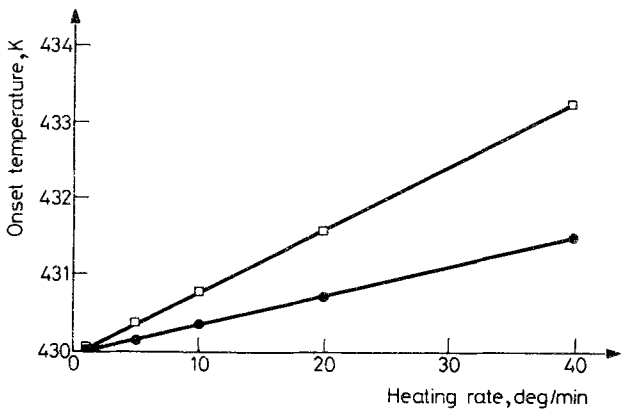

Fig. 9 Effect of heating rate on the indium onset temperature of melting with different kinds of aluminum pans. squares: hermetic pan; circles: non-hermetic crimped pan

change in melting point of indium at different heating rates. The temperature lag ΔT, caused by different heating rates (q), is almost 3 q/40 for the hermetically sealed pan and about q/40 for the non-hermetically sealed pan. One must remember, thus, that the temperature calibration does not only require measurement at a given heating rate, but also experimentation with the same kind of aluminum pan. Furthermore, it should be mentioned that a two-point temperature calibration used by the instrument software is not sufficient for precision measurement at low temperature. The calibration is not linear with temperature, as shown by the summary of data in Table 1. This problem has been recognized [5]. Recently the duPont Co. introduced a

high sensitivity DSC (DSC 2910) which has five point temperature calibration from 178 to 853 K by instrument software.

From Table 1 it can be seen that the temperature lag (ΔT) at different amplitudes depends also on the pan type and temperature. The lag ΔT is expressed as amplitude (A in mW) divided by the slope of the onset of the melting peak of the standard (φ, in mW/K). For the hermetically sealed pan, $\varphi = 2.85 + 0.0198$ x T, i.e. about 7 to 13 mW/K from 200 to 500 K. For the non-hermetically sealed pan, $\varphi = 5.272 + 0.0166$ x T, i.e. about 9 to 14 mW/K from 200 to 500 K.

Table 1 Melting point calibration

Sample	Literature	Hermetically sealed pan		Non-hermetically sealed pan	
	Melting point, K	Onset temp., K	Onset slope, mW K	Onset temp., K	Onset slope, mW K
Indium	429.8	430.8	11.5	430.3	12.4
Ice	273.2	275.8	7.9	275.3	9.9
Acetona	177.9	184.0	6.6	183.0	8.2

The temperature lag, ΔT, is thus

$$\Delta T = 3q/40 + A/(2.85 + 0.0198 \text{ x } T) \text{ for the hermetically sealed pan} \quad (3)$$

and

$$\Delta T = q/40 + A/(5.29 + 0.0166 \text{ x } T) \text{ for the non-hermetically sealed pan} \quad (4)$$

An operational problem for the hermetically sealed pan is caused by the Auto Sampler. Because the hermetically pan has a sharp edge, it may stick on the robot's fingers and sometimes cause the pan to slip out of the correct position.

The running of the low-temperature DSC without gas flow through the DSC cells to minimize the possible noise has the additional benefit that it reduces the crosstalk between cells, which was shown to depend on the gas flow rate [1].

6. The effect of heating rate differences between sample and reference

The effect of heating rate difference between sample and reference should be corrected for when calculating heat capacities from the ex-

perimental data. As was discussed in the previous papers [1, 2]. For a single-run heat capacity measurement, C_p can be expressed as follows:

$$C_{pB} = C_{pA} \times \frac{K_B \Delta T_B / q + [(K_B \Delta T_B / q + C'_p)(\mathrm{d}\Delta T_B / \mathrm{d}T_B)]}{K_A \Delta T_A / q + [(K_A \Delta T_A / q + C'_p)(\mathrm{d}\Delta T_A / \mathrm{d}T_A)]} \quad (5)$$

where C_p is the heat capacity, subscripts A and B refer to the two cell positions, K is proportional to the cell constant, q is the steady-state heating rate, ΔT is the temperature difference between reference and sample, T is the sample temperature, and C'_p is the heat capacity of the empty aluminum pan (water value).
on neglecting C'_p :

$$C_{pB} = C_{pA} \times \frac{K_B}{K_A} \times \frac{\Delta T_B}{\Delta T_A} \times \frac{(1+\mathrm{d}\Delta T_B / \mathrm{d}T_B)}{(1 + \mathrm{d}\Delta T_A / \mathrm{d}T_A)} \quad (6)$$

where K_B/K_A is the asymmetry factor discussed above. Because the DSC used records only heat flow, the relationship between temperature (ΔT) and differential heat flow (ΔHF) needed to be established first. Similar to the previous paper [1], the proportionality constants $K'$and K'' were measured and expanded to low temperature. The constant K' converts the heat flow signal in the DSC mode (in mW) to corrected mV, proportional to the temperature difference. Figure 10 shows the results for positions A and B. The curve is represented by the equation:

$$K' = -12.4867 + 0.250482 \times T - 8.61037 \times 10^{-4} \times T^2 + 2.29974 \times 10^{-6} \times T^3 - \\ -7.88903 \times 10^{-10} \times T^4 + 6.27917 \times 10^{-14} \times T^5 \quad (7)$$

with a RMS = 0.504% from 125 to 575 K. The constant K'' can be derived from the DTA mode recording and is constant (K'' = 20.0 K/mV) [1]. The conversion factor from heat flow (ΔHF) in mW to ΔT in K is thus:

$$f(T) = \Delta T / \Delta HF = K' / K'' = -0.624336 + 1.2524 \times 10^{-2} \times T - 4.3051 \times \\ \times 10^{-5} \times T^2 + 6.4986 \times 10^{-8} \times T^3 - 3.9445 \times 10^{-11} \times T^4 + 3.1395 \times 10^{-15} \times T^5 \quad (8)$$

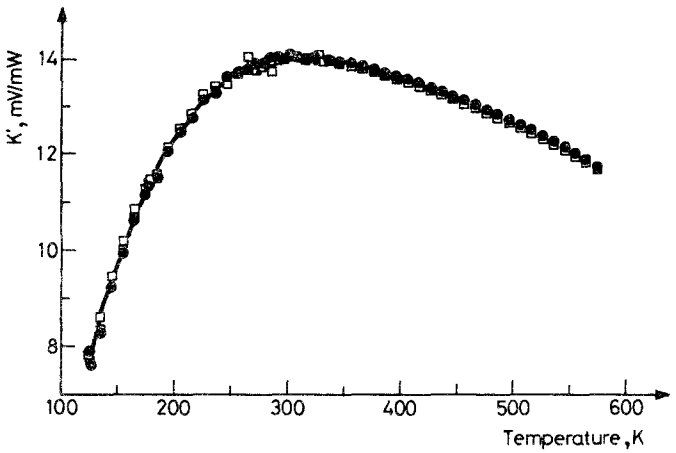

Fig. 10 Temperature dependence of signal-heat flow ratio on DSC mode. square: cell *A*; cross: cell *B*; line: fitted to Eq. (7)

As a test for the improvement of the data, we measured a sapphire standard (62.38 mg) on cell *A* and an aluminum sample (80.14 mg) on cell *B* with a 26.35 mg aluminum pan. The results and each step correction are listed in Table 2. Columns *B* and *C*: heat flow obtained by subtracting the baseline of the empty pan run from the sample run after matching the starting and ending isotherms between empty and sample runs; Column *D:* $f(T)$ calculated from Eq. (8); Columns *E* and *F*: $\Delta T = f(t)$ x Heat flow; Column *G:* literature heat capacity of sapphire [6]; column *H*: calculated heat capacity of aluminum without any corrections; Column *I:* C_p calibration constant from a previous run by using two standard sapphire samples; Column *J:* calculated heat capacity of aluminum with asymmetry correction by using the C_p calibration constant; Column *K* and *L*: slope of ΔT *vs.* T; Column *M*: partial slope correction = $(1+\mathrm{d}\,\Delta T_B/\mathrm{d}T_B)/(1+\mathrm{d}\,\Delta T_A/\mathrm{d}T_A)$, here *A* and *B* represent sapphire and aluminum, respectively; Column *N*: calculated heat capacity of aluminum with asymmetry and partial slope correction based on Eq. (6); Column *O*: water value or heat capacity of aluminum pan from previous run; Column *P:* full slope correction $= [1+(1+C'_p/C_{pB})(\mathrm{d}\,\Delta T_B/\mathrm{d}T_B)] / [1+(1+C'_p/C_{pA})(\mathrm{d}\Delta T_A/\mathrm{d}T_A)]$;
Column *Q*: calculated heat capacity of aluminum with asymmetry and full slope correction based on Eq. (5); Column *R*: literature heat capacity of aluminum [7]; Column *S*: Dev. (%) = [1 – expt. C_p/lit. C_p] x 100 %. From

Table 2 Heat capacity of aluminum with each step correction

A	B	C	D	E	F	G	H	I	J	K	L	M	N	O	P	Q	R	S
T	Heat flow		f(T)	ΔT		Heat capacity		Asymm.	C_p	dΔT/dT		Slope	C_p	C_p'	Slope	C_p of aluminum		Dev.
(K)	(mW)		(K/mW)	(K)		(J/K mol)		calib.	(J/K mol)	(K/K)		correct	(J/K mol)		correct	(J/K mol)		(%)
	Sapphire	Aluminum		Sapphire	Aluminum	Sapphire	Aluminum	K_A/K_B	Aluminum	Sapphire	Aluminum	(part)	Aluminum	Pan	(full)	(expt.)	(lit.)	
180	3.524	7.646	0.573	2.020	4.383	43.79	19.56	1.088	17.98	0.0419	0.1377	1.092	19.64	21.38	1.105	19.86	20.58	3.48
190	4.091	9.662	0.596	2.439	5.760	47.53	23.11	1.063	21.75	0.0368	0.0898	1.051	22.86	21.58	1.051	22.85	21.07	-8.47
200	4.474	10.027	0.616	2.757	6.179	51.14	23.60	1.068	22.09	0.0241	0.0258	1.002	22.12	22.21	0.994	21.95	21.53	-1.94
210	4.611	9.906	0.634	2.921	6.276	54.60	24.15	1.072	22.53	0.0206	0.0153	0.995	22.42	22.40	0.987	22.23	21.94	-1.33
220	4.888	9.999	0.648	3.170	6.484	57.92	24.39	1.070	22.80	0.0233	0.0187	0.995	22.69	22.54	0.987	22.51	22.32	-0.86
230	5.124	10.059	0.661	3.387	6.593	61.09	24.69	1.070	23.07	0.0214	0.0160	0.995	22.95	22.64	0.988	22.78	22.66	-0.54
240	5.355	10.131	0.672	3.597	6.804	64.12	24.98	1.065	23.45	0.0111	0.0028	0.992	23.25	22.74	0.987	23.13	22.97	-0.70
250	5.525	10.091	0.653	3.610	6.650	67.01	25.20	1.063	23.70	0.0192	0.0109	0.992	23.51	23.01	0.985	23.35	23.26	-0.38
260	5.793	10.218	0.687	3.982	7.023	69.75	25.33	1.061	23.87	0.0264	0.0242	0.998	23.82	23.18	0.992	23.68	23.53	-0.63
270	5.972	10.217	0.693	4.137	7.077	72.36	25.49	1.059	24.07	0.0177	0.0089	0.991	23.86	23.38	0.985	23.71	23.77	0.24
280	6.224	10.334	0.697	4.336	7.200	74.84	25.58	1.053	24.29	0.0178	0.0100	0.992	24.10	23.50	0.987	23.97	23.99	0.09
290	6.423	10.404	0.699	4.492	7.276	77.19	25.74	1.050	24.52	0.0156	0.0079	0.992	24.34	23.79	0.987	24.21	24.20	-0.06
300	6.630	10.495	0.701	4.648	7.357	79.41	25.88	1.047	24.71	0.0153	0.0082	0.993	24.54	24.11	0.988	24.42	24.38	-0.17
310	6.840	10.606	0.702	4.799	7.441	81.52	26.03	1.044	24.92	0.0126	0.0041	0.992	24.71	24.33	0.987	24.60	24.56	-0.16
320	6.987	10.609	0.701	4.899	7.439	83.50	26.10	1.038	25.14	0.0126	0.0036	0.991	24.92	24.52	0.987	24.80	24.72	-0.33
330	7.214	10.730	0.700	5.051	7.513	85.39	26.15	1.035	25.28	0.0130	0.0051	0.992	25.08	24.61	0.988	24.98	24.86	-0.46
340	7.387	10.798	0.698	5.160	7.542	87.18	26.24	1.031	25.45	0.0111	0.0026	0.992	25.23	24.77	0.988	25.13	25.00	-0.53
350	7.574	10.869	0.696	5.272	7.566	88.88	26.26	1.026	25.59	0.0095	0.0013	0.992	25.38	25.10	0.988	25.29	25.12	-0.66
360	7.717	10.915	0.693	5 350	7.567	90.52	26.36	1.023	25.77	0.0068	-0.0008	0.992	25.57	25.24	0.989	25.49	25.23	-1.01
370	7.838	10.940	0.690	5.409	7.549	92.06	26.46	1.019	25.95	0.0121	0.0025	0.991	25.71	25.47	0.986	25.60	25.34	-1.01
						Av. error	-6.45		-1.17				-1.22			-0.77		-0.77
						RMS error	±3.29		±5.57				±2.21			±2.09		±2.09

Table 3 Heat capacity of sapphire in J/(K mol)

Temperature, K	C_p Experiment	C_p Literature	Deviation, %
180	46.39	43.79	–5.61
190	47.69	47.53	–0.33
200	51.44	51.14	–0.58
210	54.72	54.60	–0.21
220	57.95	57.92	–0.06
230	61.06	61.09	0.05
240	64.36	64.12	–0.37
250	67.27	67.01	–0.39
260	69.95	69.75	–0.28
270	72.42	72.36	–0.08
280	75.11	74.84	–0.37
290	77.65	77.19	–0.59
300	79.66	79.41	–0.31
310	82.03	81.52	–0.62
320	84.00	83.50	–0.60
330	85.91	85.39	–0.61
340	87.66	87.18	–0.55
350	89.26	88.88	–0.42
360	90.99	90.52	–0.52
370	92.44	92.06	–0.41
380	93.97	93.51	–0.48
390	95.36	94.88	–0.50
400	96.41	96.18	–0.24
410	97.79	97.40	–0.39
420	99.02	98.55	–0.47
430	100.06	99.64	–0.42
440	101.06	100.69	–0.37
450	102.24	101.68	–0.55
460	103.30	102.64	–0.64
470	104.05	103.54	–0.49
480	104.87	104.42	–0.43
490	105.64	105.25	–0.37
500	106.65	106.05	–0.56
510	107.52	106.81	–0.66
520	107.81	107.55	–0.24
530	108.49	108.26	–0.21
540	109.59	108.93	–0.60
550	109.90	109.59	–0.28
560	110.89	110.21	–0.61

Average and RMS error: (–0.548±0.84)% from 180 to 56 K (–0.415±0.22)%from 190 to 560 K

column *H, J, N* and *Q,* one can see from the average ± RMS% of derivation that the calculated aluminum heat capacities gradually improve.

B. Sample C_p measurements

1. C_p of sapphire

In order to check the precision of heat capacity measurement, the following two-run experiment was done in close succession: Run 1 for baseline determination with empty pans, run 2 with granular sapphire on cell *A* and a sapphire disc on cell *B* for calibration. This was followed by a third run in the same configuration as run 2, but with a different sapphire disc which has a similar mass, now as an unknown sample, on cell *B* for C_p measurement. Table 3 shows the heat capacity of the sapphire disc as an unknown sample on cell *B*. The data were close to the literature value [7]. Average and RMS = –0.55 ± 0.84% from 180 to 500 K, or –0.42 ± 0.22% from 190 to 560 K.

Since it is the plan to measure C_p by single-run experiments, the empty pan and sapphire standard runs establish the instrument calibration constants. Subsequently one can just run the unknown sample calculate C_p from a single run, based on the prior calibration. From Fig. 7, the stability of C_p calibration constant was assured. The final question concerns thus the stability of the baseline of the empty pan run.

2. Long time baseline stability

For the single-run heat capacity measurement the baseline repeatability over a long period of time must be assured. Figures 11 and 12 show six baselines taken over the time period of more than three week (experimental dates are marked next to the curves). Changes with time, especially at low isothermal temperature range, are as big as ± 1.6 mW for cell *A* and ± 0.6 mW for cell *B*. As was seen for the high temperature range, the environment has a strong effect on the baseline repeatability.

For the low temperature range, environmental effects came mainly from two sources: one is the temperature changes and drafts outside the DSC heater jacket, the other is the liquid nitrogen coolant flow inside the DSC heater jacket. The former is more important for high temperature operation, the latter for low temperature operation. Besides controlling the room temperature, one should keep the liquid nitrogen coolant feed rate as constant as possible. This depends not only on the HEATER and RATE set-

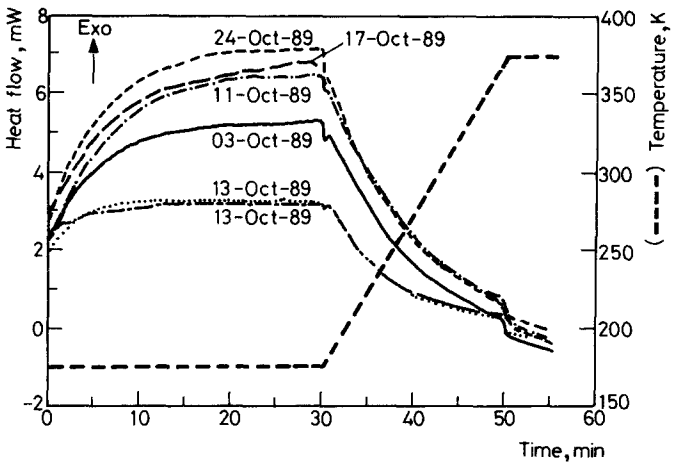

Fig. 11 Baselines of cell *A* with loading and unloading of the same aluminum pan during one month. Short dash: temperature; others: heat flow of 6 repeated runs

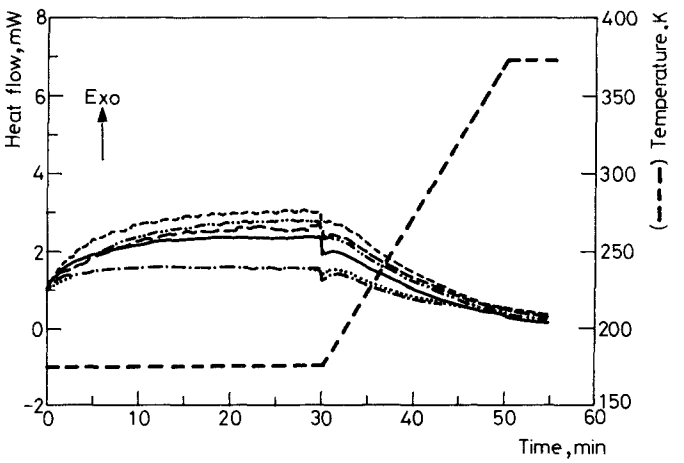

Fig. 12 Baseline of cell *B* with loading and unloading of the same aluminum pan during one month, as in Fig. 11

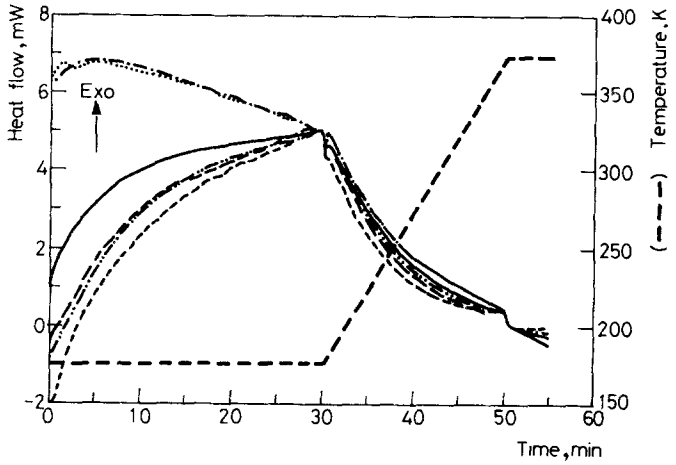

Fig. 13 Baseline of cell *A* after matched starting and ending isotherms between repeated runs, as shown in Fig. 11

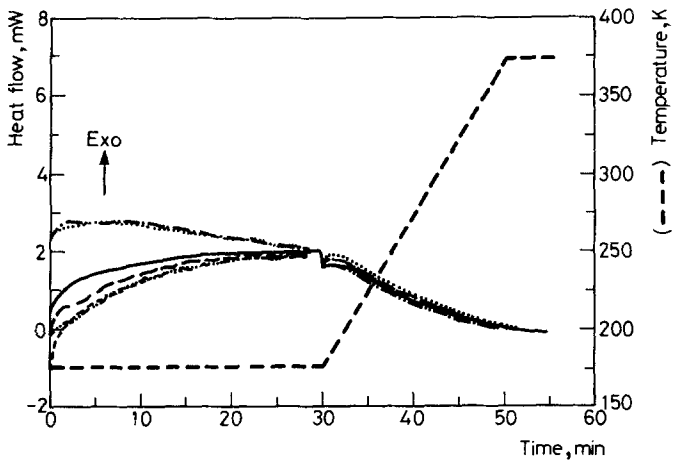

Fig. 14 Baseline of cell *B* after matched starting and ending isotherms between repeated runs, as shown in Fig. 12

Table 4 Comparison between high and low temperature experiments

Compare	High temperature, 323K	Low temperature, 173K
Peak-to-peak noise (mW)	0.028	0.250
Baseline fluctuation (mW)	±0.09(A)/0.05(B)	±0.60(A)/0.10(B)
Baseline repeatability (mW)	±0.01(A)/0.005(B)	±0.10(A)/0.040(B)
Baseline stability (mW)	±0.1	±0.3
Normal amplitude (mW)	10 to 20	5 to 10
Possible error (%)	0.5 to 1.0	3.0 to 6.0

tings, but also on the liquid nitrogen level in the tank and on the liquid nitrogen transport through the heat assembly head and tube which is, in turn, affected by room temperature. The changes are so irregular that it is best to check the isothermal baseline carefully and frequently. If one finds shifts among empty, standard, or unknown samples of less t han 2 mW for cell *A* or 1 mW for cell *B*, one might use the previous empty and standard runs to calculate heat capacity from a single run. Otherwise, it is better to rerun the empty and standard again to make sure that the changes can be corrected for.

From Figs 13 and 14 it can be seen that the maximum fluctuation of the baseline reduce to ±0.33 mW for cell *A* and ±0.13 mW for cell *B* after matching of the isothermal baseline. Again, similar as in high temperature calorimetry [1], the fluctuations of cell *A* are more than twice that of cell *B*. To reduce the experimental error, we decided to place the unknown sample on cell *B* (the right side position) and the fixed sapphire standard on cell *A* (the left side position).

3. Comparison between high and low temperature experiments

For high temperature heat capacity experiment, most errors could be controlled to within ±0.1%, except for the error caused by change of temperature of the environment. For low temperature heat capacity measurement, the instrument noise becomes higher, baseline repeatability and stability as well as heat flow amplitude become poorer compared to high temperature. Table 4 lists a comparison between high and low temperature experiments. More complicated than high temperature experiment, for low temperature experiment, liquid nitrogen control becomes important. Besides optimizing the experimental setting, some modification of the instrument will be necessary. It is hoped that this research will provide the needed scientific base for such improvements.

4. Heat capacities of five samples

Selenium, aluminum, quartz, polystyrene and sodium chloride were chosen to evaluate the instrument for the measurement of heat capacities. Table 5 shows the experimental heat capacities with asymmetry and slope correction and error of the samples when compared with literature data [8-13]. The average error and the root mean square error of all data is 0.66 ±2.86% which is in-line with the prior analysis and is quite acceptable for

Table 5 Measured heat capacities of five samples in J(Kmol)

Temp.,	Selenium		Aluminum		Quartz		Polystyrene		Sodium chloride	
K	C_p	Error*	C_p	Error*	C_p	Error*	C_p	Error*	C_p	Error*
180	21.99	3.44	18.65	10.32	33.02	–0.61	80.02	–4.84	41.64	3.20
190	23.43	–1.62	21.45	–1.74	32.34	5.73	78.82	1.52	45.17	–3.57
200	23.56	–1.02	20.94	2.80	33.91	4.51	84.25	–0.33	43.71	0.81
210	23.57	–0.05	21.08	4.09	34.82	5.05	87.56	0.54	44.09	0.94
220	23.30	2.04	21.52	3.68	35.31	6.60	89.62	2.87	44.45	0.97
230	23.51	2.05	21.87	3.63	36.83	4.89	95.42	0.60	44.53	1.51
240	23.79	1.65	22.17	3.61	37.94	4.25	100.90	–0.75	44.92	1.25
250	23.75	2.59	22.51	3.37	39.05	3.57	105.06	–0.60	45.29	0.99
260	23.94	2.41	22.87	2.87	40.33	2.38	110.36	–1.38	45.72	0.51
270	23.91	3.23	23.20	2.44	41.05	2.58	114.92	–1.37	46.48	NA
280	24.03	3.35	23.55	1.86	42.12	1.86	120.24	–1.91	48.04	NA
290	24.24	3.03	23.84	1.50	43.21	1.10	126.13	–2.79	46.96	NA
300	24.45	2.72	24.09	1.21	44.21	0.58	132.57	–3.93	47.61	NA
310	24.71	2.18	24.30	1.04	45.36	–0.28	138.24	–4.40	48.07	NA
320	24.97	1.66	24.58	0.57	46.28	–0.62	143.81	–4.74	48.64	NA
330	25.27	0.95	24.80	0.24	47.52	–1.61	148.91	–4.71	49.15	NA
340	25.55	0.33	24.96	0.15	48.60	–2.23	154.31	–4.85	49.62	NA
350	25.84	–0.36	25.12	0.01	49.68	–2.85	158.67	–4.33	50.19	NA
360	26.15	–1.04	25.29	–0.21	50.85	–3.60	162.37	–3.44	50.77	NA
370	26.42	–1.59	25.42	–0.31	51.97	–4.24	167.79	–3.56	51.48	NA

*Error = (1 - expt. Cp/lit. Cp) x 100%

Average and RMS error = (0.66±2.86)%

All experiments run from 173 to 373 K at 10 deg/min heating rate

the evaluation of heat capacities at low temperature and even somewhat better than data with the triple run instrument analyzed before [14].

* * *

This work was supported by the Division of Materials Sciences, National Science Foundation, Polymers Program, Grant # DMR 8818412 and the Division of Materials Sciences, Office of Basic Energy Sciences, U. S. Department of Energy, under Contract DE-AC05-84OR21400 with Martin Marietta Energy Systems, Inc. In addition, support by the duPont Company in acquisition of the instrumentation is acknowledged.

References

1 Y. Jin and B. Wunderlich, J. Thermal Anal., to be published.
2 B. Wunderlich, J. Thermal. Anal., 32 (1987) 1949.
3 Software written by ourself in Quick Basic to data analysis heat capacity of sample based on the paper [2].
4 DuPont Instrument Thermal Analyzers, Recommended value by DSC Calibration Data Analysis Program, Version 4.0, 1988.
5 DuPont Instruments Thermal Analyzers, (a) The TA hotline, Fall 1989 (b) Information booklet about DuPont DSC 2910.
6 D. C. Ginnings and G. T. Furukawa, J. Am. Chem. Soc., 75 (1953) 522.
7 R. L. Hultgren, "Select Values of the Thermodynamics Properties of the Elements", American Chemical Society for Metals, Ohio, 1973.
8 M. W. Chase, Jr., C. A. Davies, J. R. Downey, Jr., D. J. Frurip, R. A. McDonald and A. N. Syverud, "JANAF Thermochemical Tables" 3rd Ed., in J. Phys. Chem. Data, Vol. 14, Suppl. 1, 1985.
9 O. Kubaschewski and E. L. Evans, "Metallurgical Thermochemistry" Pergamon Press, New York 1958.
10 U. Gaur and B. Wunderlich, J. Phys. Chem. Ref. Data, 11 (1982) 313.
11 U. Gaur, H. C. Shu, A. Mehta and B. Wunderlich, ibid, 10 (19810 89.
12 H. Von Moser, Physik. Zeitschr., 37 (1936) 747.
13 I. Barin and O. Knacke, "Thermochemical Properties of Inorganic Substances" Springer-Verlag, New York 1973.
14 B. Wunderlich and U. Gaur, ACS Advances in Chemistry Series 203, Polymer Characterization, C. D. Craver, ed., Washington, DC, Pg. 195, 1983.

Zusammenfassung — In einer vorangehenden Untersuchung wurde single-run DSC zur direkten Ermittlung von Wärmekapazitätswerten angewendet. Diese Methode wird hier auf den niedrigen Temperaturbereich (180 K) ausgedehnt. Das benutzte Gerät war ein duPont Doppelproben-DSCalorimeter mit Auto-Sampler und einem Flüssigstickstoff-Kühlerzusatzgerät-II. Der größte Fehler wird durch die Niedrigtemperaturisotherme verursacht. Nach Optimierung aller Parameter wurden im Temperaturbereich 180-370 K die Wärmekapazitäten von Selen, Aluminium, Quarz, Polystyrol und Natriumchlorid gemessen. Verglichen mit der gutuntersuchten adiabatischen Kalorimetrie beträgt der Standardfehler aller Messungen ±2.9 % .

Addition in proof

After the paper: "Single run heat capacity measurement II. Experiments at subambient temperature," was completed we were made aware of a new and improved DSC cell and cellbase available from Du Pont. Through the courtesy of the company we were able to test a prototype of the updated equipment.

There are three new features to improve subambient temperature experiments. (1) A digital delta-T amplifier was installed in the cellbase in order to reduce the noise of the signal. (2) The calorimeter environment was modified by inserting insulation between the DSC furnace and the liquid nitrogen cooling head surrounding the DSC cell in order to reduce the turbulence of the gas inside the DSC furnace. (3) A special gasket which allows to purge gas past the cell connector was made to reduce the temperature gradient at the cell to cellbase connector.

These changes resulted in the following improvements:

1. The digital amplifier has a reduced noise of 1/5 of the prior level at all temperature ranges when tested with the normal cooling accessory and at the sampling interval of 0.2 s/point. For example, the peak-to-peak noise was reduced from 0.015 mW to 0.003 mW at 323 K and from 0.045 mW to 0.008 mW at 100 K.

2. The insulated cooling head reduced the baseline noise when used in the isothermal mode at different temperature. With insulation, the peak-to-peak noise at the sampling interval of 3.0 s/point was 0.005 mW, 0.015 mW, 0.04 mW, 0.09 mW, and 0.20 mW at 323 K, 273 K, 223 K, 173 K and 123 K, respectively, instead of the prior values of 0.028 mW, 0.04 mW, 0.11 mW, 0.25 mW and 0.55 mW at the respective temperatures without insulation.

3. When the nitrogen gas purge through the cellbase connector is larger than 5 psi, it reduced the baseline curvature between 123 to 373 K from 17 mW to less than 2 mW, but it increased the peak-to-peak noise at 123 K from 0.2 mW to 0.6 mW. For the improved cell and cellbase, we get the following characteristics which should be compared to Table 4 in the paper.

Among these three new features, the introduction of the new digital amplifier and the insulation reduce the baseline noise, while the connector purge reduces the baseline drift. All three changes enhance thus the performance of the instrument.

A check of Tables 4 and 4a shows that the main error comes from the baseline stability. The temperature gradient across the connector seems to be the main reason for the baseline curvature and instability at subambient temperatures. It is a simple solution to improve the baseline stability and

curvature by purging a dry gas at constant and high rate. A single bottom of nitrogen cylinder may last, however, only for about 2 runs at 5 psi.

Table 4a Comparison between high and low temperature experiments

	High temperature (323 K)	Low temperature (173 K)	
	without N_2	without N_2	with N_2 (1-2 psi)
Peak-to-peak noise (mW)	0.005	0.09	0.05
Baseline fluctuation (mW)	±0.017/±0.020	±0.35/±0.12	±0.5/±0.15
Baseline repeatability (mW)	±0.010/±0.010	±0.20/±0.06	±0.06/±0.06
Baseline stability (mW)	±0.08	±0.35	±0.25
Normal amplitude (mW)	10 to 20	5 to 10	5 to 10
Possible error (1 %)	0.4 to 0.8	3.5 to 7.0	2.5 to 5.0

Since a decreasing temperature of the connector is the main reason for the baseline shift and instability we have tried several other alterations to protect the connector, for example by using fiberglass and sponge insulation to block the cold gas from going to the connector, vent the cold nitrogen gas through a tube instead by overflow around the cellbase, put an aluminum block between jacket heater and DSC cell to keep the connector warm, etc. Some of these alterations do reduce the shift of the baseline, but still not enough for reliable and repeatable heat capacity measurements. In order to measure C_p at temperatures lower than 173 K, we found it most advantageous to use the old DSC cooling accessory instead of LNCA-II. With some simple modification of the cell and good protection of the cell base when cooling down, it is possible to repeat the isothermal baseline at 110 K. The reason for the better baseline repeatability is the quicker cooling and thus lesser conduction of heat from the cell base.

A high-sensitivity DSC with a modified connector for better subambient temperature performance has recently been introduced by Du Pont.